Discriminative Measurement for Radon Isotopes

Subjects: Others

Contributor: Chutima Kranrod, Yuki Tamakuma, Masahiro Hosoda, Shinji Tokonami

Radon and thoron measurement studies have been widely conducted and reported all over the world. Generally, the techniques used relate to the passive nuclear track detectors. Though some surveys shown that passive monitors for radon are sensitive to thoron, and hence the measured results might be probably overestimated the radon concentration. This study investigated the radon and thoron measurement in domestic and international using passive radon-thoron discriminative measuring device, commercially named RADUET. This paper attempts to provide an understanding and evident roadmap for discriminative measurements of radon isotopes.

Keywords: radon-thorn discriminative ; radon ; thoron ; RADUET

1. Introduction

Many radon surveys were conducted to investigate radon levels in the world[1][2][3][4][5][6]. Generally, a passive radon monitor is used for a large-scale survey because of its quiet and low cost. However, it was reported that some of them had a high sensitivity to thoron, which is one of its radioisotopes, and the measurement results might have been affected by the existence of thoron (^{220}Rn)[7][8][9]. The passive radon monitor which was pointed out a high sensitivity to thoron had been used for a nationwide radon survey in some countries[4][5][6][7][10]. Therefore, attention should be paid to those reported where possible thoron presence would significantly bias results for radon measurement. From a viewpoint of radiation protection, thoron was historically ignored because of its half-life (55.6 s) and difficulties in measurement and calibration. It should be noted that the quantity of thoron can be larger than that of radon in some areas such as Yangjang, China[11]. If a passive radon monitor cannot discriminatively measure radon and thoron, the measurement results will be overestimated, and it cannot be corrected due to no significant relationship between radon and thoron concentrations[8][12]. Therefore, radon and thoron should be discriminatively measured for an accurate dose assessment and future lung cancer risk assessment due to indoor radon[13].

This shows the passive radon-thoron discriminative monitors named a RADUET developed in a couple of decades.

2. Summary of RADUET

The RADUET is a passive integrated radon–thoron discriminative monitor, which was developed by Tokonami et al.[14]. Schematic drawings of the RADUET monitor are shown in Figure 1. It has double plastic chambers with different air-exchange rates or air-diffusion rates. A CR-39 (the allyl diglycol carbonate) detector, which is used to detect alpha particles emitted from radon, thoron and their progenies, is placed at the bottom of each chamber with sticky clay. The low air-exchange rate chamber is made of electro-conductive plastic with an inner volume of ~3.0 × 10^{-5} m^3. The high air-exchange rate chamber is also made of the same plastic material, but it has six holes in the wall and has an electroconductive sponge covering the holes to prevent radon and thoron decay products and aerosols from going into the chamber. Thus, radon gas can diffuse into the low air-exchange rate chamber through an invisible gap between the lid and the bottom of the chamber. Subsequently, this gap functions as a high air-diffusion rate barrier; due to its very short half-life (55.6 s), only a very small amount of thoron goes into the chamber compared to the amount for radon with a longer half-life (3.82 d). Additionally, both radon and thoron can get into the high air-exchange rate chamber. The air-exchange rates of the low and high air-diffusion rate chambers are 0.7 h^{-1} and 10 h^{-1}, respectively[15]. The air-exchange rates of RADUET chambers differ by about two orders of magnitude. Correspondingly, the difference of track density between the two CR-39s detectors from each chamber makes it possible to discriminate between radon and thoron.

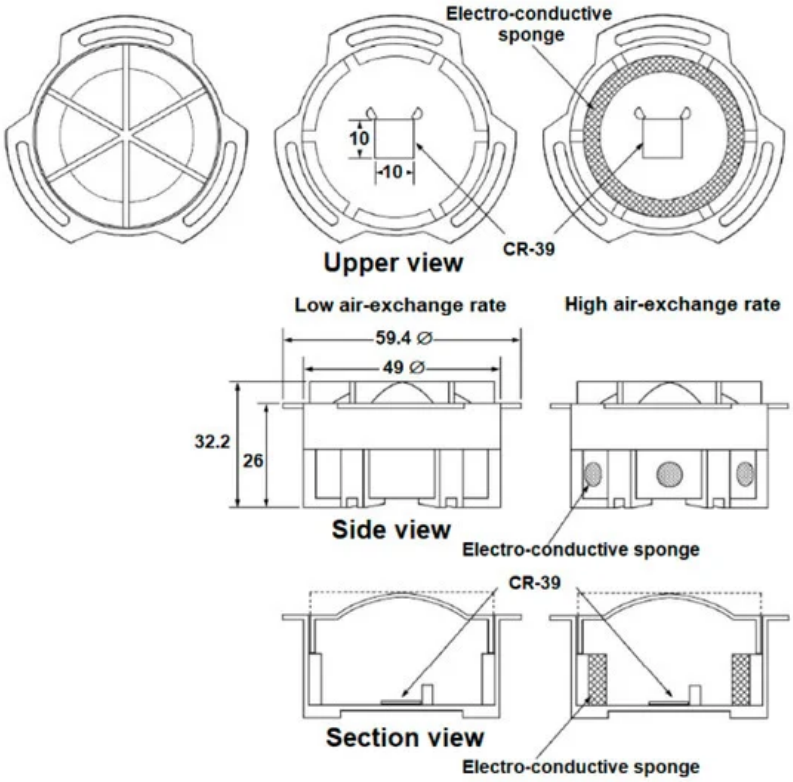

Figure 1. Schematic views of the RADUET monitor (unit: mm).

For analysis of the CR-39 detectors from the RADUET, they are chemically etched in concentrated base solution according to the manufacturers' protocols. For example, CR-39 detectors manufactured by Radosys Ltd. (Budapest, Hungary) have to be etched with a 6.25 M NaOH solution at 90 °C for 6 h, while CR-39 detectors manufactured by Nagase Landauer, Ltd. (Ibaraki, Japan) have to be etched with a 6 M NaOH solution at 60 °C for 24 h. After that, the tracks formed on CR-39 are counted with an automatic reading system or optical microscope and image software. For calculating radon and thoron concentrations, the obtained total track densities are replaced into the following equations[16]:

$$\bar{C}_{Rn} = (d_L - \bar{b}) \times \frac{f_{Tn2}}{t \times (f_{Rn1} \times f_{Tn2} - f_{Rn2} \times f_{Tn1})} - (d_H - \bar{b}) \times \frac{f_{Tn1}}{t \times (f_{Rn1} \times f1_{Tn2} - f_{Rn2} \times f_{Tn1})} \quad (1)$$

$$\bar{C}_{Tn} = (d_H - \bar{b}) \times \frac{f_{Rn1}}{t \times (f_{Rn1} \times f_{Tn2} - f_{Rn2} \times f_{Tn1})} - (d_L - \bar{b}) \times \frac{f_{Rn2}}{t \times (f_{Rn1} \times f1_{Tn2} - f_{Rn2} \times f_{Tn1})} \quad (2)$$

where $\bar{C}_{Rn}$ and $\bar{C}_{Tn}$ are the mean concentrations of radon and thoron during the exposure period in Bq m^{-3}. d_L and d_H are the total alpha track densities (track m^{-2}) taken from the CR-39 detectors of low and high air-exchange rate chambers. f_{Rn1} and f_{Tn1} are the radon and thoron calibration coefficients for the low air-exchange rate chamber in tracks m^{-2} kBq^{-1} m^3 h^{-1}. f_{Rn2} and f_{Tn2} are the radon and thoron calibration coefficients for the high air-exchange rate chamber in tracks m^{-2} kBq^{-1} m^3 h^{-1}. t is the exposure time in hours and $\bar{b}$ is the background track density of the CR-39 detector in tracks m^{-2}.

Remark: The low air-exchange rate chamber limits diffusion of thoron into the chamber, therefore, $f_{Rn1} >> f_{Tn1}$. The high air-exchange rate chamber is designed such that both radon and thoron can diffuse into the chamber easily, and $f_{Rn2} \sim f_{Tn2}$.

To determine the calibration coefficients, RADUETs should be calibrated at a reference laboratory. The calibration coefficients are estimated by a correlation between the track density and the time-integrated radon and thoron concentrations from three or four exposure levels of radon and thoron[17]. In the calibration procedure of the radioactive gas monitor, most RADUET monitors are calibrated using a secondary method based on a calibration via a reference monitor. Thus, five to ten monitors, depending on the size of the calibration chamber, are placed in the middle of the chamber for each reference exposure condition. The introduction level of radon and thoron in each calibration chamber should be assigned to three or four different levels for the time-integrated radon and thoron concentrations such as ~500 kBq h m^{-3}, ~1000 kBq h m^{-3}, ~2000 kBq h m^{-3} and ~3000 kBq h m^{-3}. These calibrations are intended to obtain traceability to primary standards of radon isotopes and to test linearity of monitor response over the whole range of interest of exposure values. Throughout the calibration experiments, concentration of radon isotopes in the chamber is

continuously monitored with active measurement equipment which has itself been compared with a standard for radon isotopes. Moreover, environmental parameters, such as humidity, pressure and temperature in the calibration chamber should be continuously measured and constantly observed. After exposure, the CR-39 detectors from RADUET are chemically etched and afterwards the number of tracks on the CR-39 is counted as used for measurement samples. In addition, the background noise from five or ten CR-39 detectors that have not been exposed to radon and thoron and have been processed under the same chemical etching and counting conditions are measured at the same time as the calibration. Subsequently, the four calibration curves are plotted as the time-integrated radon or thoron exposure (on the X axis) versus the track density (on the Y axis) for the high and low air-exchange rates of RADUET. Thus, f_{Rn1}, f_{Tn1}, f_{Rn2} and f_{Tn2} are given by fitting each calibration curve using linear regression[14]. The slope of the linear line of each calibration curve is the calibration coefficient or calibration factor between the density of the tracks per unit of time (tracks m^{-2} h^{-1}) and the activity concentration (kBq m^{-3}) of the reference atmosphere.

Moreover, based on the fact of the RADUET that concentration in one chamber depends on the other, the calculation procedure for the decision threshold and detection limits are estimated in the following manner [16]. The decision thresholds of the average radon concentration and the average thoron concentration are obtained from Equations (1) and (2) and their standard uncertainty for $\widetilde{C}_{Rn} = 0, \bar{u}(d_L) = 0, \widetilde{C}_{Tn} = 0$ and $\bar{u}(d_H) = 0.$ These yield Equations (3) and (4). (It should be noted that α= 0.05 and $k_{1-\alpha}$ = 1.65 are often selected by default.)

$$\bar{C}^{*}_{Rn} = k_{(1-\alpha)}.\bar{u}(0) = k_{(1-\alpha)}\sqrt{(\omega_1^2 u^2(\bar{b}\,) - 2\omega_1\omega_2 u^2(\bar{b}\,) + \omega_2^2(u^2(d_H) + u^2(\bar{b}\,)) + \frac{(d_H^2 - 2\bar{b}\,d_H + b^2)\omega_2^2}{\omega_1^2}u^2(\omega_1) + (-d_H + \bar{b}\,)^2 u^2(\omega_2)} \quad (3)$$

$$\bar{C}^{*}_{Tn} = k_{1-\alpha}.\bar{u}(0) = k_{1-\alpha}\sqrt{(\omega_3^2 u^2(\bar{b}\,) - 2\omega_3\omega_4 u^2(\bar{b}\,) + \omega_4^2(u^2(d_L) + u^2(\bar{b}\,)) + \frac{(d_L^2 - 2\bar{b}\,d_L + \bar{b}^{\,2})\omega_4^2)}{\omega_3^2}u^2(\omega_3) + (-d_L + \bar{b}\,)^2 u^2(\omega_4)} \quad (4)$$

The detection limit of the average radon ($\bar{C}^{**}_{Rn}$)and thoron concentration ($\bar{C}^{**}_{Tn}$) are calculated as given in Equations (5) and (6). (It should be noted that α = β = 0.05 and $k_{1-\alpha}$ = $k_{1-\beta}$ = 1.65 are often selected by default.)

$$\bar{C}^{**}_{Rn} = \bar{C}^{*}_{Rn} + k_{1-\beta}.\bar{u}\left[\bar{C}^{**}_{Rn}\right] = \bar{C}^{*}_{Rn} + k_{1-\beta}\sqrt{(\omega_1^2[u^2(d_L) + u^2(\bar{b}\,)] - 2\omega_1\omega_2 u^2(\bar{b}\,) + \omega_2^2[(u^2(d_H) + u^2(\bar{b}\,)] + \frac{(d_H^2 - 2\bar{b}\,d_H + \bar{b}^{\,2})\omega_2^2 + C^{-}_{R}n(2d_H - 2\bar{b}\,)\omega_(2) + C^{-}_{R}n^2)}{\omega_1^2}u^2(\omega_1) + (-d_H + \bar{b}\,)^2 u^2(\omega_2)} \quad (5)$$

$$\bar{C}^{**}_{Tn} = \bar{C}^{*}_{Tn} + k_{1-\beta}.\bar{u}\left[\bar{C}^{**}_{Tn}\right] = \bar{C}^{*}_{Tn} + k_{1-\beta}\sqrt{(\omega_3^2[u^2(d_H) + u^2(\bar{b})] - 2\omega_3\omega_4 u^2(\bar{b}\,) + \omega_4^2[(u^2(d_L) + u^2(\bar{b}\,)] + \frac{(d_L^2 - 2\bar{b}\,d_L + \bar{b}^{\,2})\omega_4^2 + C^{-}_{T}n(2d_L - 2\bar{b}\,)\omega_(4) + C^{-}_{T}n^2)}{\omega_1^2}u^2(\omega_3) + (-d_L + \bar{b}\,)^2 u^2(\omega_4)} \quad (6)$$

Here $\omega 1 = \frac{f_{Tn2}}{t \times (f_{Rn1} \times f_{Tn2} - f_{Rn2} \times f_{Tn1})}$, $\omega 2 = \frac{f_{Tn1}}{t \times (f_{Rn1} \times f_{Tn2} - f_{Rn2} \times f_{Tn1})}$, $\omega 3 = \frac{f_{Rn1}}{t \times (f_{Rn1} \times f_{Tn2} - f_{Rn2} \times f_{Tn1})}$ and $\omega 4 = \frac{f_{Rn2}}{t \times (f_{Rn1} \times f_{Tn2} - f_{Rn2} \times f_{Tn1})}$ are the true values of the average radon and thoron concentrations. $\bar{u}\,(d_L)$ and $\bar{u}\,(d_H)$ are the standard uncertainties of the estimators of $\bar{C}_{Rn}$ and $\bar{C}_{Tn}$, $\bar{u}\left[\bar{C}^{**}_{Rn}\right]$ and $\bar{u}\left[\bar{C}^{**}_{Tn}\right]$ are the standard uncertainties of detection limits of average radon and thoron concentrations associated with measurement results.

Based on the calculation procedure given above, the detection limits for the typical measurement conditions have been estimated in the literature to be 3 Bq m^{-3} for radon and 14 Bq m^{-3} for thoron[14]. Moreover, the detection limits for the high background area condition have been assessed to be 10 Bq m^{-3} for radon and 20 Bq m^{-3} for thoron[18].

3. Conlusion

The advantages of the radon-thoron discriminative monitor known as the RADUET were reviewed and as well the strategic plans for regional and national surveys in various countries. Most were regional surveys of indoor radon and thoron measurements.

References

1. United Nations Scientific Committee on the Effects of Atomic Radiation, UNSCEAR 2006 Report, Effects of ionizing rad iation. Volume I: Annex E Sources-to-effects assessment for radon in homes and workplaces. UNSCEAR, NewYork, 20 09.
2. Sanada, T.; Fujimoto, K.; Miyano, K.; Doi, M.; Tokonami, S.; Uesugi, M.; Tanaka, Y. Measurement of nationwide indoor Rn concentration in Japan. 1999, 45: 129-137.

3. Wang, Z.; Lubin, J. H.; Wang, L.; Zhang, S.; Boice, Jr., J. D.; Cui, H.; Zhang, S.; Conrath, S.; Xia, Y.; Shang, B.; Brenner, A.; Lei, S.; Metayer, C.; Cao, J.; Chen, K. W.; Lei, S.; Kleinerman, R. A. Residential radon and lung cancer risk in a high-exposure area of Gansu province, China. Am. J. Epidmiol. 2002, 155(6): 554-564.
4. Wichman, H. E.; Rosario, A. S.; Heid, I. M.; Kreuzer, M.; Heinrich, J.; Kreienbrock, L. Increased lung cancer risk due to residential radon in a pooled and extended anlysis of studies in Germany. Health Phys. 2005, 88(1): 71-79.
5. Krewski D.; Lubin, J. H.; Zielinski, J. M.; Alavanja, M.; Catalan, V. S.; Field, R. W. A combined analysis of north Amarican case-control studies of residential radon and lung cancer. J. Toxicol. Environ. Health A 2007, 69(7-8): 533-597.
6. Dowdall, A.; Murphy, P.; Pollard, D.; Fenton, D. Update of Ireland's national average indoor radon concentration - Application of a new survey protocol. J. Environ. Radioact. 2017, 169-170: 1-8.
7. Park, T. H.; Kang, D. R.; Park, S. H.; Yoon, D. K.; Lee, C. M. Indoor radon concentration in Korea residential environments. Environ. Sci. Pollut. Res. 2018, 25: 12678-12685.
8. Ivanova, K.; Stojanovska, Z.; Kunovska, B.; Chobanova, N.; Badulin, V.; Benderev, A. Analysis of the spatioal variation of indoor radon concentrations (national survey in Bulgaria). Environ. Sci. Pollut. Res. 2019, 26: 6971-6979.
9. Tokonami, S.; Yang, M.; Sanada, T. Contribution from thoron on the response of passive radon detectors. Health Phys. 2001, 80(6): 612-615.
10. Tokonami, S. Why is 220Rn (thoron) measurement important? Radiat. Prot. Dosim. 2010, 141: 335-339.
11. Omori, Y.; Hosoda, M; Takahashi, F.; Sanada, T.; Hirao, S.; Ono, K.; Furukawa, M. Japanese population dose from natural radiation. J. Radiol. Prot. 2020, in press, available at https://iopscience.iop.org/article/10.1088/1361-6498/ab73b1.
12. Fujimoto, K.; Kobayashi, K.; Uchiyama, M.; Doi, M.; Nakamura, Y. Nationwide indoor radon survey in Japan. Jpn. J. Health Phys. 1997, 32(1): 41-51 (in Japanese with English abstract).
13. International Commission on Radiological Protection, Occupational intakes of radionuclides: Part 3. ICRP Publication 137, Ann. ICRP 46(3/4), ICRP, New York, 2017.
14. Tokonami, S.; Takahashi, H.; Kobayashi, Y.; Zhuo, W. Up-to-date radon-thoron discriminative detector for a large-scale survey. Rev. Sci. Instrum. 2005, 76, 113505.
15. Omori, Y.; Tamakuma, Y.; Nugraha, E.D.; Suzuki, T.; Saputra, M.A.; Hosoda, M.; Tokonami, S. Impact of Wind Speed on Response of Diffusion-Type Radon-Thoron Detectors to Thoron. Int. J. Environ. Res. Public Health 2020, 17, 3178.
16. International Organization for Standards, Measurement of radioactivity in the environment-Air-Radon 220: Integrated measurement methods for the determination of the average activity concentration using passive solid-state nuclear track detectors ISO16641, ISO, Geneva, 2014.
17. Pornnumpa, C.; Oyama, Y.; Iwaoka, K.; Hosoda, M.; Tokonami, S. Development of radon and thoron exposure systems at Hirosaki University. Radiat. Environ. Med. 2018, 7(1), 13-20.
18. Bineng, G.S.; Saïdou; Tokonami, S.; Hosoda, M.; Tchuente Siaka, Y.F.; Issa, H.; Suzuki, T.; Kudo, H.; Bouba, O; The Importance of Direct Progeny Measurements for Correct Estimation of Effective Dose Due to Radon and Thoron. Front Public Health. 2020, 8, 17.
